Energy Proceedings
Vol 34, 2023
ISSN 2004-2965

Establishment of computational model for CO_2 experimental pipeline charging process based on equal-density principle

Shuai Yu[1], Xingqing Yan[1], Yifan He[1], Jianliang Yu[1*]

1 Dalian University of Technology, No 2 Ling Hong Road, Dalian 116024, China.

(*Corresponding Author: yujianliang@dlut.edu.cn)

ABSTRACT

The sustainable deterioration of the climate caused by continuous global warming poses a serious threat to human survival. Carbon Capture Utilization and Storage (CCUS) is a potential and effective technology to alleviate global warming. CO_2 pipeline transportation is an economical and safety way to connect other parts in the CCUS system. It is essential to understand the characteristics of CO_2 release and hazards and these are essential to the design and arrangement of pipeline. Existent CO_2 pipeline release experimental studies lack of repeatable verification tests, especially those seriously affected by the environment, CO_2 far-field diffusion research, for example. It is necessary to guarantee the same initial conditions between different repetitive tests. In this paper, the equal density principle for CO_2 pipeline release tests was summed up based on thermal process before release operation. A computational model to calculate the charging mass and phase state of CO_2 to achieve a specific initial pressure and temperature inside pipeline for release test was established, using MTLAB software. The Span-Wagner (SW) equation of state was applied to calculate the thermodynamic properties of CO_2. The initial pressure, initial temperature, and inventory in authors' previous studies are presented. By comparing the experimental data and the calculated results, the model has good predictive ability. Larger CO_2 mass for the injection operation is the result of lower initial temperature or greater initial pressure. The numerical model provides convenience to improve accuracy for CO_2 release tests.

Keywords: CCUS; Pipeline transportation; CO_2 release; Numerical model; Thermodynamics.

1. INTRODUCTION

Carbon Capture, Utilization and Storage (CCUS) is one latest technology to deal with global warming (Rodrigues et al., 2022). CCUS is a developing technology and every link face security challenge. In the CCUS system a significant number of CO_2 was captured from atmosphere or emission source and transported to specific areas to utilize or storage by pipeline(Balaji and Rabiei, 2022). However, several factors like pipelines corrosion, construction defects, mechanical damage, etc. may pose the leakage risk to CO_2 pipeline(Teng et al., 2021).

Han et al. (2013), Xie et al. (2014), Vree et al. (2015) and Yamasaki et al. (2017) conducted a number of CO_2 decompression experiments. Existing CO_2 pipeline release experimental research, particularly those that are substantially impacted by the environment, such as CO_2 far-field diffusion study, need repeatable verification testing. The identical initial circumstances must be ensured during various repeating tests. This paper summarized the equal-density principle based on the test procedure in author's studies. A numerical model is established based on Span-Wagner (SW) state equation(Span and Wagner, 1996).

2. NUMERICAL MODELING

2.1 SW state equation

The Span-Wagner (SW) (Span and Wagner, 1996) equation of state is applied to calculate the thermodynamic property of CO_2. It is widely used in the thermodynamic property calculation for many fluids because of high accuracy(Flechas et al., 2020; Lemmon and Span, 2006). The deviation function calculation method is adopted for S-W equation. The dimensionless Helmholtz energy for actual fluid $\varphi(\delta, \tau)$ is equal to the

This is a paper for International CCUS Conference 2023 (ICCUSC2023), April 14-15, 2023, Beijing, China.

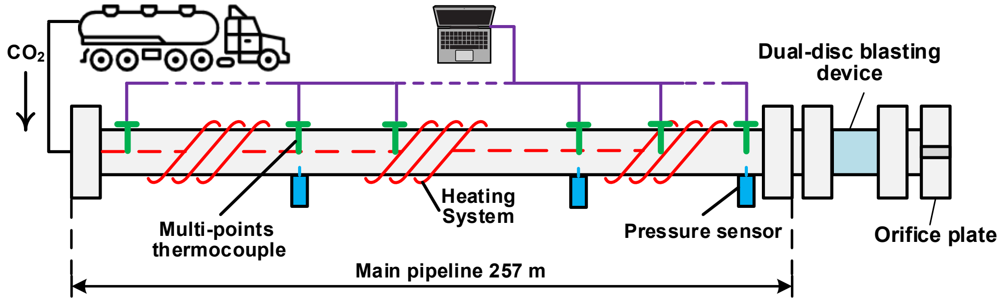

Fig. 1. Schematic diagram of industry-scale experimental apparatus.

sum of ideal-fluid behavior $\varphi^0(\delta,\tau)$ and residual fluid behavior $\varphi^r(\delta,\tau)$:

$$\varphi(\delta,\ \tau)=\varphi^0(\delta,\ \tau)+\varphi^r(\delta,\ \tau) \tag{1}$$

$$\varphi^0(\delta,\ \tau)=\ln(\delta)+a_1^0+a_2^0\tau+a_3^0\ln(\tau)+\sum_{i=4}^{8}a_i^0\ln\left[1-\exp\left(-\tau\theta_i^0\right)\right] \tag{2}$$

$$\varphi^r(\delta,\ \tau)=\sum_{i=1}^{7}n_i\delta^{d_i}\tau^{t_i}+\sum_{i=8}^{34}n_i\delta^{d_i}\tau^{t_i}e^{-\delta^{c_i}}+\sum_{i=35}^{39}n_i\delta^{d_i}\tau^{t_i}e^{-\alpha(\delta-\varepsilon_i)^2-\beta_i(\tau-\gamma_i)^2}+\sum_{i=40}^{42}n_i\Delta^{b_i}\delta e^{-C_i(\delta-1)^2-D_i(\tau-1)^2} \tag{3}$$

$$\Delta=\left\{(1-\tau)+A_i\left[(\delta-1)^2\right]^{1/(2\beta_i)}\right\}^2+B_i\left[(\delta-1)^2\right]^{a_i} \tag{4}$$

where $\delta=\rho/\rho_c$ is the reduced density and $\tau=T/T_c$ is the inverse reduced temperature. ρ and T are the density and temperature of CO_2 respectively. ρ_c and T_c are the critical density and critical temperature of CO_2 respectively. A_i, B_i, C_i, D_i, a_i, a_i^0, b_i, c_i, d_i, n_i, τ_i, α_i, β_i, γ_i, ϑ_i^0, and ε_i are the fitting coefficients, as shown in APPENDIX A.

The relation of density to dimensionless Helmholtz energy consisting of and is given by:

$$\rho(\delta,\tau)=\frac{P}{RT\left(1+\delta\varphi_\delta^r\right)} \tag{5}$$

$$\varphi_\delta^r=\left(\frac{\partial\varphi^r}{\partial\delta}\right)_\tau \tag{6}$$

where R is specific gas constant of CO_2 and P is the pressure of CO_2. The calculation methods of other thermodynamic parameters are described in detail by Span et al(Span and Wagner, 1996) and not mentioned in this study.

2.2 Equal-density principle

The industry-scale experimental apparatus included a 257 m long main pipeline, two injection pipes, heating system and dual-disc blasting device. It is shown in Fig. 1. The inner diameter and thickness of main pipeline was 233 m and 20 mm respectively. The texture of main pipeline was 16MnR steel. The two injection pipes on the one end of main pipeline were used to inject gas phase and liquid phase CO_2. The dual-disc blasting device was on the release end of pipeline and the texture was 304 stainless steel. According to the pressure different, it will commence the CO_2 release. The maximum operation pressure of the experimental apparatus is 16 MPa. There was a 1200 m long heating tape and a 50 mm thick cotton insulation around main pipeline tightly. They were used to heat CO_2 to meet experimental initial condition. Based on the experimental design, a replaceable flange was used to install on the release end, which were 15 mm. Huge recoil generated during the release. Therefore, a reinforcing device was designed and installed at the release end of pipeline to protect whole experimental apparatus.

The test procedure in author's studies(Guo et al., 2016b, 2016a) shows that when the appropriate mass of CO_2 was added to the pipe, all inlet valves and venting valve were shut down. The total mass of CO_2 inside the pipeline would not change before release. Besides, it is obvious that the volume of pipeline (V) was not changed. The equal-density principle refers to the density of CO_2 inside the pipeline remained equal throughout the period between finishing CO_2 injection to release operation. Besides, before release operation, the initial pressure and initial temperature (P_0 and T_0) inside the pipeline can determine the initial density (ρ_0). Combined with the density and the volume of the pipe, the total mass of CO_2 inside the pipeline before release (M_{re}) for the injection operation required to achieve the initial temperature and initial pressure can be calculated. Based on equal-density principle, the volume fraction of the saturated liquid phase and the saturated gas phase can be determined. And for the CO_2 injection operation, the CO_2 was fed into the pipeline using a tank car with gas–liquid CO_2 of 2.2 MPa and -10°C (P_{in} and T_{in}). The density of saturation liquid and saturation gas ($\rho_{in\text{-}L}$ and $\rho_{in\text{-}G}$) can be calculated by P_{in} and T_{in}. based on SW equation. Further, the required mass of saturation liquid ($M_{in\text{-}L}$) and saturation gas ($M_{in\text{-}G}$) can be determined combined with M_{re}. The calculation flow chart of numerical model is Fig. 2, where $\alpha_{in\text{-}G}$ and $\alpha_{in\text{-}L}$ are the volume fraction of liquid CO_2 and gas CO_2, respectively. M_{in} is the total injection mass of liquid CO_2 and gas CO_2 for the injection operation.

3. RESULTS AND DISCUSSION

3.1 Model verification

Table. 1 shows the temperature, pressure and the total mass of CO_2 inside the pipeline before release

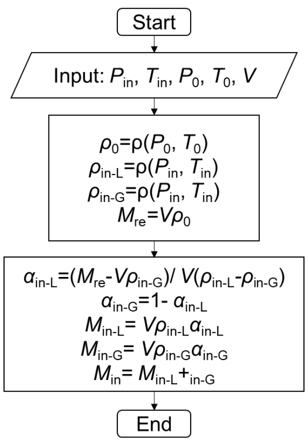

Fig. 2. Calculation flow chart of numerical model.

operation for Test 1-Test 9. The experimental initial conditions are presented in author's previous studies (Test 1-Test 6 in Guo et al. (2016a), Test 7-Test 9 in Guo et al. (2016b)). The inventory was obtained by weight difference of the tank car before and after injection operation. Table. 2 shows the calculation results for the injection operation for Test 1-Test 9. In the numerical model, the density of saturation liquid CO_2 and saturation gas CO_2 are 1016.0 kg/m^3 and 58.3 kg/m^3, respectively. The total volume of pipeline is 10.96 m^3. For Test 1, the measure inventory of CO_2 was 0.97 tons. And the calculation injection mass at 2.2 MPa and -10^{o}C is 0.95 tons with a volume fraction of saturation liquid CO_2 for 0.032. The required mass of saturation liquid CO_2 is 0.34 tons. It is obvious that the calculation required inventory for injection operation is near equal with the measure inventory before release in the tests by comparing the data in all of the tests in Table. 1 and Table. 2. It can be concluded that once the initial temperature and pressure of the test are determined, the mass of the CO_2 required for the injection operation can be determined based on equal-density principle. It is convenient to repeat a series of tests with the same initial conditions.

3.2 Case study

Fig. 3 shows the influence of initial pressure (7.5, 8.0, 8.5, 9.0, 9.5 and 10.0 MPa before release) on total inventory, required mass of saturation liquid ($M_{in\text{-}L}$) and

Table.1 The temperature, pressure and the total mass of CO_2 inside the pipeline before release operation for Test 1-Test 9.

No.	P_0 (MPa)	T_0 (°C)	Inventory (tons)
Test 1	4.05	33.8	0.97
Test 2	4.00	33.4	0.96
Test 3	3.60	32.7	0.84
Test 4	9.2	17.4	9.48
Test 5	9.1	19.3	9.31
Test 6	9.1	21.6	9.11
Test 7	7.6	35.1	3.14
Test 8	7.9	33.4	6.27
Test 9	8.0	36.9	3.59

Table. 2 The numerical results after injection operation (2.2 MPa, -10°C) for Test 1-Test 9.

No.	$\alpha_{in\text{-}G}$	$M_{in\text{-}G}$ (tons)	$\alpha_{in\text{-}L}$	$M_{in\text{-}L}$ (tons)	Inventory (tons)
Test 1	0.968	0.61	0.032	0.34	0.95
Test 2	0.969	0.62	0.031	0.33	0.95
Test 3	0.981	0.65	0.019	0.21	0.86
Test 4	0.157	0.10	0.843	9.39	9.49
Test 5	0.173	0.11	0.827	9.21	9.32
Test 6	0.192	0.12	0.808	9.00	9.12
Test 7	0.761	0.49	0.239	2.66	3.15
Test 8	0.472	0.30	0.528	5.88	6.18
Test 9	0.719	0.46	0.281	3.13	3.59

volume fraction of saturation liquid ($\alpha_{in\text{-}L}$) for the injection operation. The initial temperature is set to 35^{o}C. The injection conditions are set to 2.2 MPa and -10^{o}C, gas-liquid phase, similar to test conditions. The volume of pipeline is 10.96 m^3. It can be seen that with the increasing of initial pressure, to reach the setting initial pressure and temperature, more inventory and saturation liquid are required. At the same time, the volume fraction of liquid phase in gas-liquid two-phase

flow increases gradually. It is because the density of CO_2 is proportional to the pressure, at constant temperature.

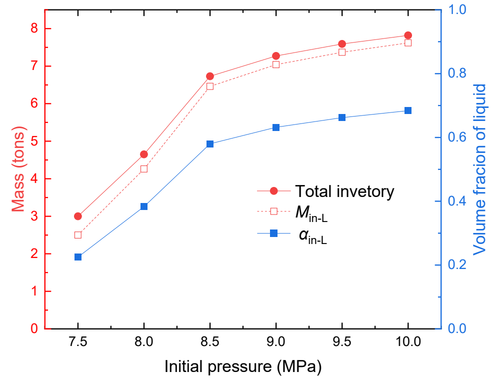

Fig. 3. Influence of initial pressure on the parameters for injection operation.

Fig. 4 shows the influence of initial temperature (15°C, 20°C, 25°C, 30°C, 35°C and 40°C before release) on total inventory, required mass of saturation liquid ($M_{in\text{-}L}$) and volume fraction of saturation liquid ($\alpha_{in\text{-}L}$) for the injection operation. The initial pressure is set to 8.0 MPa. The injection conditions are also similar to test conditions. It can be seen that with the increasing of initial temperature, to reach the setting initial pressure and temperature, less inventory and saturation liquid are required. At the same time, the volume fraction of liquid phase in gas-liquid two-phase flow decreases gradually. It is because the density of CO_2 is inversely proportional to the temperature, at constant pressure.

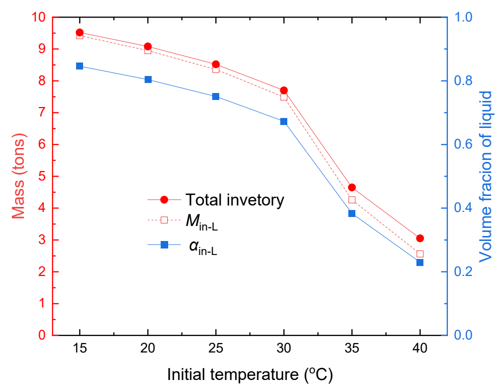

Fig. 4. Influence of initial temperature on the parameters for injection operation.

4. CONCLUSIONS

This study presents the development of a numerical model based on the equal-density principle and SW state equation. Through the comparison of experimental results and calculation, the calculation mass of CO_2 required in the whole experiment process is accurate. Lower initial temperature or higher initial pressure results in larger CO_2 mass for the injection operation. The equal-density approach can be used to calculate the mass of CO_2 required for the injection operation to reach that the target temperature and pressure of the test have been determined. Repeating a set of tests under the same initial circumstances is convenient by the numerical model.

APPENDIX A

Coefficients of Eq. 2:

i	a_i^0	ϑ_i^0
1	8.37304456	0
2	-3.70454304	0
3	2.50000000	0
4	1.99427042	3.15163
5	0.62105248	6.11190
6	0.41195293	6.77708
7	1.04028922	11.32384
8	0.08327678	27.08792

Coefficients of Eq. 3:

i	n_i	d_i	t_i
1	0.38856823203161	1	0
2	2.93854759427400	1	0.75
3	-5.58671885349340	1	1.00
4	-0.76753199592477	1	2.00
5	0.31729005580416	2	0.73
6	0.54803315897767	2	2.00
7	0.12279411220335	3	0.75

i	n_i	d_i	t_i	c_i
8	2.16589615432200	1	1.50	1
9	1.58417351097240	2	1.50	1
10	-0.23132705405503	4	2.50	1
11	0.05811691643144	5	0	1
12	-0.55369137205382	5	1.50	1
13	0.48946615909422	5	2.00	1
14	-0.02427573984350	6	0	1
15	0.06249479050168	6	1.00	1
16	-0.12175860225246	6	2.00	1
17	-0.37055685270086	1	3.00	2
18	-0.01677587970043	1	6.00	2
19	-0.11960736637987	4	3.00	2
20	-0.04561936250878	4	6	2
21	0.03561278927035	4	8.00	2
22	-0.00744277271321	7	6.00	2
23	-0.00173957049024	8	0	2
24	-0.02181012128953	2	7.00	3
25	0.02433216655924	3	12.00	3
26	-0.03744013342346	3	16.00	3
27	0.14338715756878	5	22.00	4
28	-0.13491969083286	5	24.00	4
29	-0.02315122505348	6	16.00	4
30	0.01236312549290	7	24.00	4
31	0.00210583219729	8	8.00	4
32	-0.00033958519026	10	2.00	4
33	0.00559936517716	4	28.00	5
34	-0.00030335118056	8	14.00	6

i	n_i	d_i	t_i	α_i	β_i	γ_i	ε_i
35	-213.65488688320	2	1.00	25	325	1.16	1
36	26641.56914927200	2	0	25	300	1.19	1
37	-24027.21220455700	2	1.00	25	300	1.19	1
38	-283.41603423999	3	3.00	15	275	1.25	1
39	212.47284400179	3	3.00	20	275	1.22	1

i	n_i	a_i	b_i	β_i	A_i	B_i	C_i	D_i
40	-0.66642276540751	3.500	0.875	0.3	0.7	0.3	10	275
41	0.72608632349897	3.500	0.925	0.3	0.7	0.3	10	275
42	0.05506866861284	3.000	0.875	0.3	0.7	1	12.5	275

ACKNOWLEDGEMENT

The authors would like to acknowledge the funding received from the National Key Research and Development Program of China "Intergovernmental Cooperation in In-ternational Science and Technology Innovation" Project (2019YFE0197400).

DECLARATION OF INTEREST STATEMENT

The authors declare that they have no known competing financial interests or personal relationships that could have appeared to influence the work reported in this paper. All authors read and approved the final manuscript.

REFERENCE

[1] Balaji, K., Rabiei, M., 2022. Carbon dioxide pipeline route optimization for carbon capture, utilization, and storage: A case study for North-Central USA. Sustain. Energy Technol. Assessments 51, 101900. https://doi.org/10.1016/j.seta.2021.101900

[2] Flechas, T., Laboureur, D.M., Glover, C.J., 2020. A 2-D CFD model for the decompression of carbon dioxide pipelines using the Peng-Robinson and the Span-Wagner equation of state. Process Saf. Environ. Prot. 140, 299–313. https://doi.org/10.1016/j.psep.2020.04.033

[3] Guo, X., Yan, X., Yu, J., Yang, Y., Zhang, Y., Chen, S., Mahgerefteh, H., Martynov, S., Collard, A., 2016a. Pressure responses and phase transitions during the release of high pressure CO_2 from a large-scale pipeline. Energy 118, 1066–1078. https://doi.org/10.1016/j.energy.2016.10.133

[4] Guo, X., Yan, X., Yu, J., Zhang, Y., Chen, S., Mahgerefteh, H., Martynov, S., Collard, A., Proust, C., 2016b. Pressure response and phase transition in supercritical CO_2 releases from a large-scale pipeline. Appl. Energy 178, 189–197. https://doi.org/10.1016/j.apenergy.2016.06.026

[5] Han, S.H., Kim, J., Chang, D., 2013. An experimental investigation of liquid CO_2 release through a capillary tube. Energy Procedia 37, 4724–4730. https://doi.org/10.1016/j.egypro.2013.06.381

[6] Lemmon, E.W., Span, R., 2006. Short fundamental equations of state for 20 industrial fluids, Journal of Chemical and Engineering Data. https://doi.org/10.1021/je050186n

[7] Rodrigues, H.W.L., Mackay, E.J., Arnold, D.P., 2022. Multi-objective optimization of CO_2 recycling operations for CCUS in pre-salt carbonate reservoirs. Int. J. Greenh. Gas Control 119, 103719. https://doi.org/10.1016/j.ijggc.2022.103719

[8] Span, R., Wagner, W., 1996. A new equation of state for carbon dioxide covering the fluid region from the triple-point temperature to 1100 K at pressures up to 800 MPa. J. Phys. Chem. Ref. Data 25, 1509–1596. https://doi.org/10.1063/1.555991

[9] Teng, L., Liu, X., Li, X., Li, Y., Lu, C., 2021. An approach of quantitative risk assessment for release of supercritical CO_2 pipelines. J. Nat. Gas Sci. Eng. 94, 104131. https://doi.org/10.1016/j.jngse.2021.104131

[10] Vree, B., Ahmad, M., Buit, L., Florisson, O., 2015. Rapid depressurization of a CO_2 pipeline - an experimental study. Int. J. Greenh. Gas Control 41, 41–49. https://doi.org/10.1016/j.ijggc.2015.06.011

[11] Xie, Q., Tu, R., Jiang, X., Li, K., Zhou, X., 2014. The leakage behavior of supercritical CO_2 flow in an experimental pipeline system. Appl. Energy 130, 574–580. https://doi.org/10.1016/j.apenergy.2014.01.088

[12] Yamasaki, H., Yamaguchi, H., Hattori, K., Neksa, P., 2017. Experimental Observation of CO_2 Dry-ice Behavior in an Evaporator/Sublimator. Energy Procedia 143, 375–380. https://doi.org/10.1016/j.egypro.2017.12.699